Prediction of Adipose Tissue Composition Using Raman Spectroscopy: Average Properties and Individual Fatty Acids

J. Renwick Beattie[a], Steven E.J. Bell[a,*], Claus Borgaard[b], Ann Fearon[c], and Bruce W. Moss[c]

[a]School of Chemistry, Queen's University, Belfast BT9 5AG, Northern Ireland, [b]Danish Meat Research Institute, 4000 Roskilde, Denmark, and [c]School of Agriculture and Food Science, Queen's University, Belfast BT9 5AG, Northern Ireland

ABSTRACT: Raman spectroscopy has been used for the first time to predict the FA composition of unextracted adipose tissue of pork, beef, lamb, and chicken. It was found that the bulk unsaturation parameters could be predicted successfully [R^2 = 0.97, root mean square error of prediction (RMSEP) = 4.6% of 4 σ], with *cis* unsaturation, which accounted for the majority of the unsaturation, giving similar correlations. The combined abundance of all measured PUFA (≥2 double bonds per chain) was also well predicted with R^2 = 0.97 and RMSEP = 4.0% of 4 σ. *Trans* unsaturation was not as well modeled (R^2 = 0.52, RMSEP = 18% of 4 σ); this reduced prediction ability can be attributed to the low levels of *trans* FA found in adipose tissue (0.035 times the *cis* unsaturation level). For the individual FA, the average partial least squares (PLS) regression coefficient of the 18 most abundant FA (relative abundances ranging from 0.1 to 38.6% of the total FA content) was R^2 = 0.73; the average RMSEP = 11.9% of 4 σ. Regression coefficients and prediction errors for the five most abundant FA were all better than the average value (in some cases as low as RMSEP = 4.7% of 4 σ). Cross-correlation between the abundances of the minor FA and more abundant acids could be determined by principal component analysis methods, and the resulting groups of correlated compounds were also well-predicted using PLS. The accuracy of the prediction of individual FA was at least as good as other spectroscopic methods, and the extremely straightforward sampling method meant that very rapid analysis of samples at ambient temperature was easily achieved. This work shows that Raman profiling of hundreds of samples per day is easily achievable with an automated sampling system.

Paper no. L9812 in *Lipids 41*, 287–294 (March 2006).

Government dietary guidelines in the United Kingdom (UK) are based on the assumption that nutritional or dietary management, and in particular management of dietary lipid intake, can help reduce mortality and morbidity from cardiovascular disease (CVD). At present, UK Department of Health guidelines (1994) recommend that the contribution of lipid intake to total dietary energy should be reduced from about 40 to 30% of dietary energy intake and that the contribution from saturated FA in particular should be reduced from 15 to 10% of total energy intake (1). They also recommend that the ratio of PUFA to saturated FA in the diet should be increased (1). Many studies have identified the involvement of a high intake of saturated fat with increased risk of CVD (2–4), and specific saturated FA are now recognized to have hypercholesterolemic effects. In a review of studies investigating the cholesterolemic effects of individual FA, Kris-Etherton and Yu (5) concluded that the saturated FA 12:0–16:0, were hypercholesterolemic but that the unsaturated FA were hypocholesterolemic, with PUFA being more potent than monounsaturated FA. The essential n-3 FA, such as 18:3 α-linolenic acid, have also been demonstrated to have health benefits by lowering blood lipid concentrations and reducing the risk of platelet aggregation and thrombosis (6). Finally, in recent years there has been much interest and research on the potential health benefits of consumption of CLA, and the anticarcinogenic and antiatherosclerotic properties of some isomers of CLA have been demonstrated in animal studies and models (7–10).

The net result of all the foregoing is that it is becoming increasingly important to measure the abundance of individual FA in the complex mixtures of lipids that are found in foods. This is particularly true for samples that have been deliberately treated to move their FA composition away from "typical" values. For example, the saturated nature of animal lipids has adversely influenced their perception by consumers; this has led to research aimed at reducing the high level of saturated FA and increasing the proportion of PUFA in both meat and milk lipids through dietary manipulation (11–14).

This paper is part of a series that investigate the feasibility of applying Raman spectroscopy to the analysis of FA-based fats and oils (15–18). In previous experimental studies, the correlation between particular bands in the Raman spectra of solid and liquid samples of pure FAME (15) and properties such as average chain length was investigated. This experimental work on FAME was complemented by density functional calculations, which allowed the underlying reasons for the experimentally determined structure/spectra correlations to be explored (16,17). Application of the same approach to real foodstuffs (clarified butterfat) showed that even with mixed TG, rather than simple model FAME, bulk composition parameters, e.g., chain length or iodine value, could be determined from Raman spectra (18). Furthermore, in addition to bulk or average properties, it was also possible to build multivariate calibration models that allowed the abundance of individual FA to be determined (18). The ability to monitor levels of desirable/undesirable components is obviously important in dietary lipids.

*To whom correspondence should be addressed. E-mail: S.Bell@QUB.ac.uk

Abbreviations: CVD, cardiovascular disease; GC, gas chromatograph/chromatography; PCA, principal component analysis; PLS, partial least squares; RMSEP, root mean square error of prediction; UK, United Kingdom.

Here we extend the work on butterfat to investigation of adipose tissue; the aim is to find whether Raman spectra can still be used to predict FA composition when the samples are drawn from a much broader range of sources, including tissue from different species.

EXPERIMENTAL PROCEDURES

Samples. The samples used in this investigation were subcutaneous adipose tissue dissected from above the *Longisimus dorsi* in the position of the 12th rib for beef, lamb, and pork, and from above the breast for chicken. As it is well known that the FA composition varies between the inner and outer surfaces of adipose tissues, care was taken when dissecting the samples to note the outer (next to skin) and inner (next to muscle) surfaces of the adipose tissue. Samples were obtained from a number of research sources and were all dissected within 48 h of slaughter.

GC. GC was the primary analysis method in this study. Subsamples (*ca.* 0.2–0.5 g) of adipose tissue were dissected from the regions, on each surface of the samples, that had been Raman probed. These samples were then extracted three times in 10 mL of 2:1 chloroform/methanol. FAME were prepared from the extracted fat according to the British Standard method (British Standards Institute BS 684-2.34) and were analyzed by GC (18). Aliquots of FAME in heptane (0.1 μL) were injected *via* a septa programmable injector at 250°C onto a GC column (WCOT CP Sil-88; i.d. 0.25 mm; length 50 m; film thickness 0.2 μm) supplied by Varian Inc. (Middelburg, The Netherlands) fitted in a Varian 3400 gas chromatograph (GC). An FID was used, and the heating program was ramped as follows to improve separation of the FA peaks: 50°C for 1.0 min, 50 to 140°C at 20°C min^{-1}, 140 to 225°C at 5°C min^{-1}, and finally 225°C for 10.0 min. Pure FAME, obtained from Sigma-Aldrich (Poole, UK), were used to prepare internal and external standards to establish retention times and peak identification. The following acids, as well as all FA 20 carbons in length, were undetectable in at least one species: 12:0, 14:1*c*Δ9, 15:1*c*Δ10, 17:1*c*Δ10, and 18:2*t*Δ9,12. Only FA detectable in more than half the samples were investigated. The total combined abundance of PUFA was determined by summing the relative abundances of all the PUFA including those only detected in pork and chicken (half of the samples).

Raman spectroscopy. Raman measurements were carried out using a 785 nm excitation wavelength (typically 100–120 mW at the sample, 10 cm^{-1} resolution, 180° geometry) generated by a home-built spectrometer previously described (19). Raman spectra of 8–10 samples of each of the four species were recorded. The sample was mounted on a rotating stage, oriented with the surface perpendicular to the incident radiation. The laser was line focused on the surface of the sample while the stage was rotated, giving an approximate coverage of 1.5 cm^2. Spectra were accumulated from both sides (outer and inner) to give two separate spectra for each sample, yielding a total of 16–20 spectra per species. Wavelength calibration was carried out using a neon emission lamp. The spectrograph was calibrated for Raman shift using a 50:50 (vol/vol) acetonitrile/toluene mixture [comparing to frequency standards from the American Standard Testing Method (ASTM E 1840 (1996)]. The Raman signal was recorded from 270 to 1900 cm^{-1}, the region containing the C–C, C=C, C–O and C=O, stretches and the C–H bends, in two sequential 60-s accumulations.

The non-Raman background in the raw data was removed, and the spectra were normalized and mean-centered as previously described (18). Standard partial least squares (PLS) analysis was carried out between the Raman data and FA profiles (using PLS2 to simultaneously model the full range of FA) using The Unscrambler™ v9.1 (Camo, Trondheim, Norway) and leave-one-out cross-validation to confirm the predictive ability of the model generated. During the PLS analysis of the data the Uncertainty Test was used to select the wavenumber shifts correlated with the measured parameter and reject wavenumber shifts not contributing to the prediction. To test the predictive ability of the models on unknown samples, calibrations were generated using PLS2 with test set validation. The data set was prepared by removing a subset of 10 randomly selected spectra and the model constructed from the remaining 63 samples and validated using the subset of 10. All species were represented in the test set.

RESULTS AND DISCUSSION

Figure 1 shows the average Raman spectrum of adipose tissue from each of the species used in this experiment. The major bands have been assigned previously, but for convenience they are numbered on the Figure and the most important assignments are given in Table 1. The differences between the average adipose tissue spectrum of each species, as shown in Figure 1, are larger than the differences between the butterfats obtained under various feeding regimes that were studied previously (18). The average FA profiles of the four species studied and the corresponding average bulk properties are given in Tables 2 and 3, respectively. The data in Figure 1 show that the samples are partly melted because the spectra show features similar to those characteristic of both liquid FAME (which give only broad unresolved features in several spectral regions) and solid FAME (which typically display sets of narrow, well-defined bands (15). The differences between solid and liquid FAME are particularly noticeable at *ca.* 1000–1200 cm^{-1}, and in the spectra shown in Figure 1 there are sharp solid-phase peaks on top of underlying broad liquid-phase bands in this spectral range.

Since the Raman spectra contain readily identifiable bands associated with particular groups, such as C=C bonds or CH_2 groups, it would be expected that the Raman spectrum of a mixed sample, being an ensemble average of the spectra of the individual FA chains present, would reflect the bulk sample properties. For example, the determination of unsaturation (measured as C=C per chain or per gram, i.e., in molar or molal units, respectively) is the most widely investigated aspect of the Raman spectra of lipids. In the adipose tissue samples investigated here, the level of unsaturation (the number of *cis* un-

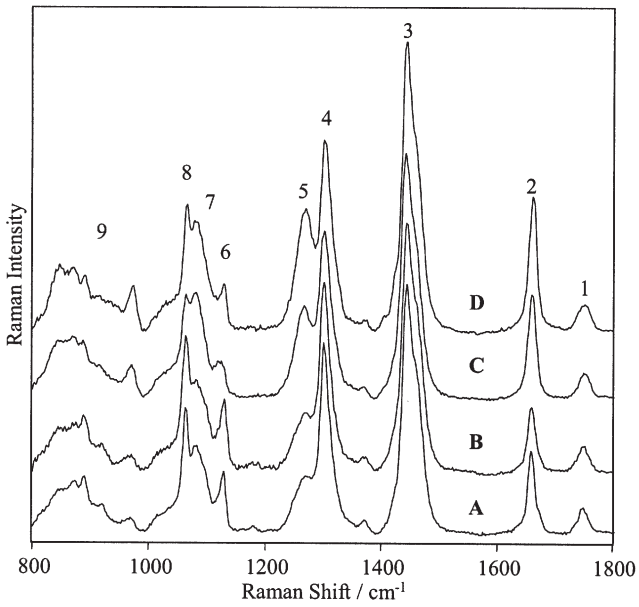

FIG. 1. Average Raman spectra for each species: (A) beef, (B) lamb, (C) chicken, and (D) pork. The numbering of the bands refers to the band positions and assignments given in Table 1. Each average spectrum has been normalized about the carbonyl stretch band at *ca.* 1750 cm^{-1}. Spectra acquired at 19–21°C.

saturated bonds per chain, i.e., molar unsaturation) was well-predicted using standard PLS2 methods, which gave a correlation coefficient of $R^2 = 0.97$ and a root mean square error of prediction (RMSEP) of 4.6% of the range. In contrast, it was not possible to find a good prediction model for *trans* unsaturation; the best model gave $R^2 = 0.52$ and RMSEP = 18% of the range. This poor *trans* prediction ability is due to the low range of relative abundances of *trans* unsaturated bonds in the adipose tissue (0.031, compared with 0.24 bonds per FA for *cis* unsaturated bonds). However, it has previously been demonstrated that Raman spectroscopy is capable of accurately predicting *trans* content in samples with a larger range of *trans* values (20). Total unsaturation (sum of *cis* and *trans*) was predicted with similar accuracy to the *cis* content, primarily because the low *trans* unsaturation meant that it was the well-predicted *cis* contribution that dominated total unsaturation.

In addition to unsaturation, another major compositional parameter is the average chain length. It was found that, as was the case for butterfats and model FAME, the Raman spectra could be used to predict average chain length satisfactorily, $R^2 = 0.92$ and RMSEP = 6.9% of the range. Since the chain length is the sum of the number of saturated and unsaturated C–C bonds and both chain length and unsaturation were modeled satisfactorily in this sample set, it would be expected that the third parameter, number of saturated C–C bonds, could also be modeled. However, it was found that even the best model gave an unsatisfactory correlation, $R^2 = 0.58$, for the average number of C–C bonds per chain. Although this result appears anomalous, it is a straightforward consequence of the fact that the number of saturated bonds per chain varied very little between samples ($\sigma = 0.07$, compared with 0.24 for unsaturated bonds), which made it difficult to model. In effect, the number of saturated bonds was almost constant in all the tissue samples so that modeling the increase in double bonds effectively also measured the increase in chain length over a constant baseline value of *ca.* 15.5 saturated C–C bonds per chain. In sample sets with a larger range of saturated C–C values it should be possible to obtain a better calibration.

The ability to predict bulk composition parameters from Raman spectra is not surprising if the spectra of individual FA are simply regarded as the sum of the contributions from individual entities, because incremental structural changes would be expected to give incremental increases in the intensities of the associated vibrational bands. For example, addition of CH_2 groups into the chain would be expected to increase the intensities of the vibrations associated with the methylene groups, such as the CH_2 twist and scissoring bands. However, if this model were strictly accurate, it would be impossible to determine relative proportions of the individual constituents in samples containing mixtures of different FA since there would be many ways of preparing different mixtures with the same bulk properties, which would therefore give the same overall spectrum. However, experimental and theoretical studies on model FAME showed that, whereas many of the vibrational modes did show the expected incremental changes with changing structure, there were some bands that did not follow a smooth progression and potentially might allow the variation in indi-

TABLE 1
Assignment of Bands in the Raman Spectra of Adipose Tissue at Ambient Temperature (19–21°C)

Band[a]	Band position (cm^{-1})	Assignment (ref.)
1	1730–1750	ν (C=O) Carbonyl stretch (27)
2	1670–1680	*trans* ν (C=C) Olefinic stretch (28)
	1650–1660	*cis* ν (C=C) Olefinic stretch (28)
3	1400–1500	$\delta\,(CH_2)_{sc}$ Methylene scissor deformations (27)
4	1295–1305	$\delta\,(CH_2)_{tw}$ Methylene twisting deformations (29)
5	1250–1280	$\delta\,(=CH)_{ip}$ In-plane *cis* olefinic hydrogen bend (29)
6	1100–1135	$\nu\,(C–C)_{ip}$ In-phase aliphatic C–C stretch *all trans* (30)
7	1080–1090	$\nu\,(C–C)_{g}$ Liquid: aliphatic C–C stretch in *gauche* (31)
8	1060–1065	$\nu\,(C–C)_{op}$ Out-of-phase aliphatic C–C stretch all-*trans* (32)
9	800–920	$\nu\,(C_1–C_2)$, $CH_{3\ rk}$, ν (C–O) Complex broad table in liquid (33)

[a]The band number refers to the numbering in Figure 1.

TABLE 2
Average FA Profile of Each of the Animal Species Used to Prepare the Calibration for the Raman Spectra

FA	Lamb[a]	Beef[a]	Pork[a]	Chicken[a]
14:0	4.18	4.09	1.16	0.79
14:1*c*Δ9	1.26	1.47	ND[a]	0.19
15:0	0.65	1.20	ND	0.12
16:0	28.83	28.74	20.46	23.23
16:1*c*Δ9	5.00	5.67	1.67	5.80
17:0	1.08	1.17	0.33	0.12
17:1*c*Δ10	0.95	ND	0.22	0.25
18:0	13.91	11.95	10.39	5.47
18:1*c*Δ9	37.53	39.37	32.70	45.05
18:1*t*[b]	2.53	1.97	0.09	0.78
18:2*c*Δ9,12	1.03	2.18	26.55	14.90
18:2*t*Δ9,12	0.26	2.19	ND	ND
18:3*c*Δ6,9,12	0.19	ND	0.09	0.27
18:3*c*Δ9,12,15	0.57	ND	2.60	1.99
20:0	0.21	ND	0.16	0.02
20:xc[c]	1.58	ND	3.47	0.88

[a]Values quoted are g/100 g FA. ND = not detected.
[b]The isomers for 18:1*t* are not well resolved, so the figure is for an undifferentiated mixture of isomers.
[c]The various 20-carbon unsaturated FA could not be unambiguously assigned under experimental conditions, and so have been grouped together.

TABLE 3
The Average Chemical Subunit Content[a] for Each of the Species, Derived from the Subset Used for GC Analysis

Parameter (per chain)	Species	Average	SD
Total number of Carbons (no. of C)	Beef	16.576	0.044
	Pork	16.375	0.077
	Chicken	16.117	0.029
	Lamb	16.024	0.055
Total number of saturated bonds (no. C–C)	Beef	15.599	0.042
	Pork	15.528	0.017
	Chicken	15.488	0.007
	Lamb	15.436	0.037
Total number of unsaturated bonds (no. C=C)	Pork	1.030	0.076
	Chicken	0.903	0.020
	Beef	0.572	0.038
	Lamb	0.548	0.059
trans:cis Ratio (%)	Beef	13.341	7.818
	Lamb	6.080	2.019
	Chicken	0.872	0.096
	Pork	0.089	0.049

[a]For each chemical subunit the samples are arranged in descending order.

TABLE 4
Regression Coefficients and Standard Errors of Prediction for the Prediction of FA Content and Bulk Parameters Using Raman Spectra

				RMSEP[d]				No.	No.
	Mean[a]	σ[b]	R^2 [c]	Absolute[d]	(% Mean)[d]	(% 4 σ)[d]	RMSEE[e]	samples	Factors
14:0	2.55	1.66	0.793	0.751	29.5	11.3	0.494	72	4
14:1*c*Δ9	0.71	0.74	0.472	0.517	72.7	17.5	0.416	53	4
15:0	0.5	0.48	0.823	0.202	40.3	10.5	0.063	72	4
16:0	25.3	4.08	0.892	1.304	5.2	8.0	1.362	72	1
16:1*c*Δ9	4.51	2.03	0.834	0.804	17.8	9.9	0.684	72	3
17:0	0.68	0.5	0.819	0.21	30.8	10.5	0.150	72	3
17:1*c*Δ10	0.47	0.36	0.7	0.206	43.9	14.3	0.054	54	5
18:0	10.46	3.78	0.89	1.257	12	8.3	1.403	72	3
18:1*c*Δ9	38.61	5.48	0.796	2.476	6.4	11.3	1.842	72	2
18:1*t*[f]	1.371	1.56	0.752	0.81	59.1	13.0	0.843	63	4
18:2*c*Δ9,12	11.18	10.99	0.965	2.058	18.4	4.7	2.278	72	3
18:2*t*Δ9,12	1.25	1.13	0.613	0.719	57.5	15.9	0.597	38	3
18:3*c*Δ9,12,15	1.71	0.93	0.932	0.284	16.6	7.6	0.205	54	3
18:3*c*Δ6,9,12	0.18	0.09	0.593	0.053	29.7	14.7	0.030	54	6
20:0	0.13	0.1	0.719	0.055	42.5	13.8	0.029	54	4
20-Carbon unsaturated[g]	1.977	1.190	0.890	0.392	19.8	8.2	0.45	54	5
Chain length	17.3	0.23	0.922	0.063	0.4	6.9	0.054	73	3
Saturation	15.51	0.07	0.575	0.046	0.3	16.3	0.037	73	3
Unsaturation	0.76	0.22	0.965	0.041	5.4	4.6	0.033	73	3
cis Unsaturation	0.73	0.24	0.965	0.045	6.2	4.7	0.041	73	3
trans Unsaturation	0.026	0.031	0.516	0.022	82.7	17.9	0.020	73	3
cis/trans	5.1	6.57	0.499	4.66	91.4	17.7	3.81	73	8
PUFA[h]	17.3	12.64	0.973	2.01	11.6	4.0	2.54	56	3
Group 1	12.46	34.8	0.971	2.07	16.6	5.9	2.32	73	3
Group 2	42.94	28.4	0.861	2.70	6.3	9.5	3.76	73	7
Group 3	6.35	12.6	0.926	2.00	31.6	15.8	1.96	73	2
Group 4	1.27	3.4	0.925	0.30	23.8	9.0	0.42	73	7
Group 5	10.77	18.0	0.884	1.31	12.2	7.3	1.62	73	3

[a]Mean weight percentage of total FA (g/100 g FA) for all samples used within investigation.
[b]SD of the % total mass of lipid from the mean.
[c]Least squares regression correlation coefficient (validation).
[d]Root Mean SE of prediction (RMSEP) as absolute value and as percentage of mean (RMSEP % of μ) and sample range (RMSEP % of 4 σ).
[e]Root Mean SE of estimate (RMSEE), determined by test set validation, removing a subset of 10 samples.
[f]The isomers for 18:1*t* are not well resolved, so the figure is for an undifferentiated mixture of isomers.
[g]These FA are unassigned due to difficulty in unambiguously identifying the different 20-carbon unsaturated FA under the experimental conditions used in this study.
[h]PUFA represents the combined abundances of all measured FA with ≥2double bonds in the chain. FA groups, as determined by grouping in principal components analysis: Group 1 = 18:3*c*Δ9,12,15; 18:2*c*Δ9,12; 20:xa ; Group 2 = 18:2*t*Δ9,12; 18:1*c*Δ9, 18:3Δ6,9,12; 16:1*c*Δ9; Group 3 = 16:0, 18:1*t*Δ9; 15:0, 17:1*c*Δ10; 14:0; 14:1*c*Δ9; 17:0; Group 4 = 20:xb; 20:xc*; Group 5 = 20:0, 18:0. *Here the symbols 20xa–c stand for three different 20-carbon FA, which could be distinguished in the GC but could not be unambiguously identified.

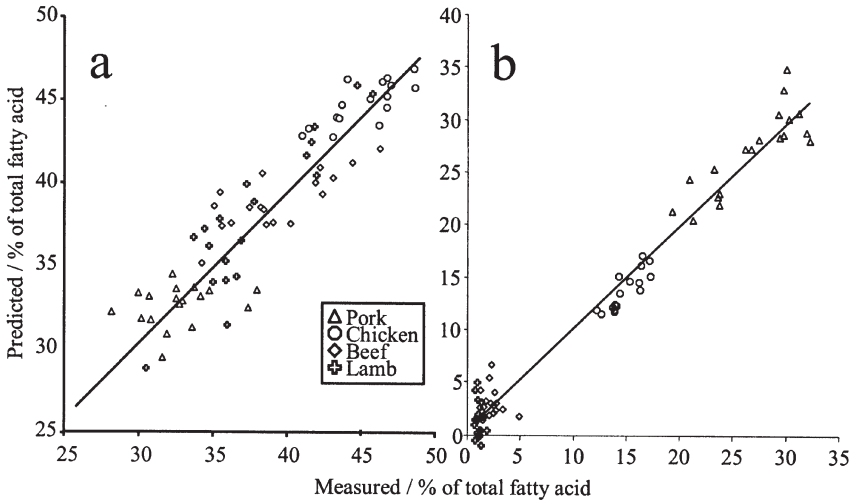

FIG. 2. Partial least squares (PLS) regression validation plot for (a) percentage of 18:1*c*Δ9 and (b) percentage of 18:2*c*Δ9,12 compared with total FA content (g/100 g FA) in subcutaneous adipose tissue predicted from Raman spectra against the percentage of total FA measured by GC.

vidual constituents to be determined, even in mixed samples with the same bulk composition (15,17).

Previously it was found that PLS1 regressions of Raman data against the amounts of individual FA in butterfat samples (18) (determined by GC as percentage of total FA) could be used to predict the relative proportions of the major FA in butterfat. In the previous study PLS1 regressions were used to create individual calibration models for each FA; in this study PLS2 was used so that we could generate a single model that predicted all the FA in the profile. The PLS2 approach gives slightly reduced prediction accuracy but it is preferable owing to its inherent simplicity. Table 4 shows the results for a PLS2 regression carried out for 73 samples of subcutaneous adipose tissue. The samples were taken from four different species, which ensured the extent of variation of each individual FA was acceptably large, but they were not separated according to

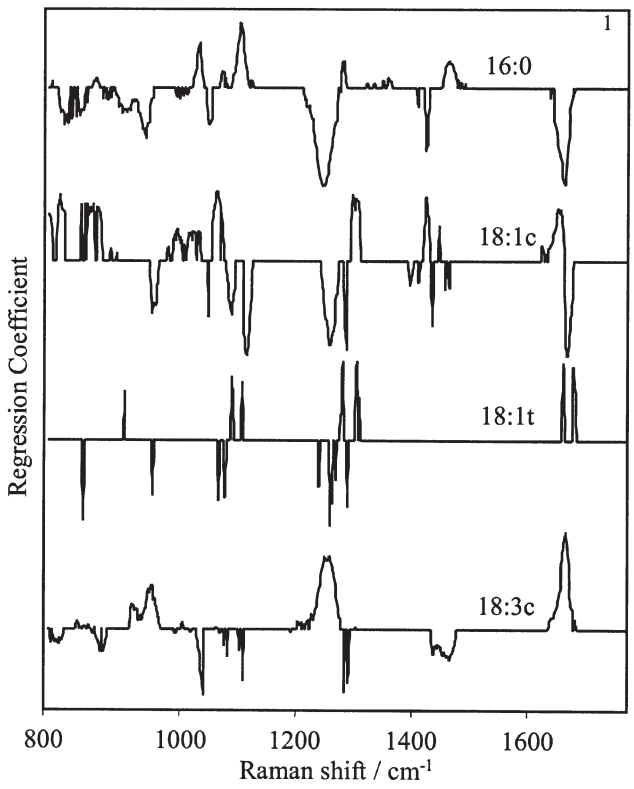

FIG. 3. PLS regression coefficients used to predict, from the Raman spectra of intact tissue at 19–21°C, the percentage of total FA content of 16:0, 18:1*c*Δ9, 18:1*t*, and 18:3*c*Δ9,12,15 in subcutaneous adipose tissue, as determined by GC. For abbreviation see Figure 2.

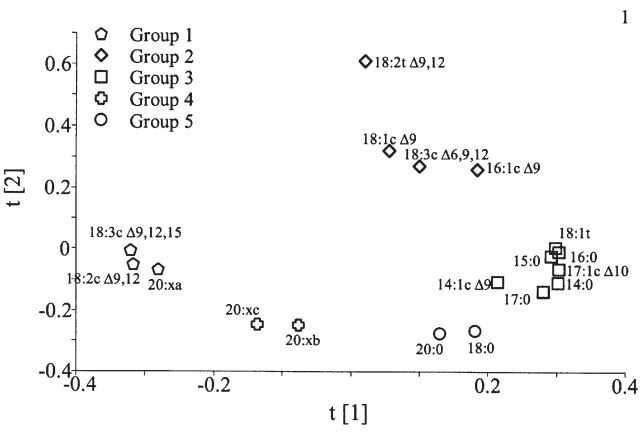

FIG. 4. Principal components analysis loading plot for the GC data, showing the groups of interrelated FA present in adipose tissue. Group 1 = 18:3*c*Δ9,12,15, 18:2*c*Δ9,12,20xa; Group 2 = 18:2*t*, 18:1*c*Δ9, 18:3*c*Δ6,9,12, 12:0, 16:1*c*Δ9; Group 3 = 16:0, 18:1*t*, 15:0, 17:1*c*Δ10, 14:0, 14:1*c*Δ9, 17:0; Group 4 = 20:xb 20:xc; Group 5 = 20:0, 18:0. Here the symbols 20xa–c stand for three different 20-carbon FA, which could be distinguished in the GC but could not be unambiguously identified.

species for the purpose of regression. The Table shows that the four most abundant FA analyzed had regression correlation coefficients ranging from R^2 = 0.80 to 0.97, with standard errors of prediction ranging from 4.7 to 11.3% of the range (4 σ). Example regression plots of the most common FA (18:1*c*Δ9) and that of the FA with the largest range (18:2*c*Δ9,12) are shown in Figure 2. Of all the moderately abundant (>3%) FA, 18:1*c*Δ9 gave the poorest correlation (due to the relatively narrow range of values, range = 14% of the mean, compared with 98% of the mean for 18:2*c*Δ9,12) but it is clear from Figure 2 that even in this worst case the scatter in the plot is still reasonably small with no systematic error apparent. This is reflected in the prediction error of 6.4% of the mean, which is acceptably low for a rapid, nondestructive analytical method. These FA are of particular interest as they confer the predominant chemical and physical characteristics of the lipids within the adipose tissue and furthermore have important consequences in health and nutrition. For example, 16:0 is known to be hypercholesterolemic, whereas the *cis* unsaturated acids lower cholesterol (in particular, LDL).

The loadings used to predict the proportion of selected FA from the Raman spectrum are presented in Figure 3. The pattern of bands used to predict each FA agrees well with well-established assignments of the bands in the Raman spectrum of FAME. The saturated FA 16:0 has positive correlation coefficients in positions known to arise from saturated modes (e.g., 1440, 1300, 1130, and 1060 cm^{-1}) whereas bands related to unsaturated modes are negative (e.g., 1270 and 1660 cm^{-1}). Conversely, the unsaturated FA would be expected to have positive coefficients for unsaturated modes and negative coefficients for saturated modes. The weighting plot for 18:3*c*Δ9,12,15 shows the expected pattern, such as large positive bands at 1660 (*cis* C=C stretch) and 1270 cm^{-1}. The 18:1*t* FA shows some of the expected bands such as positive bands at the *trans* C=C stretch position (1670–1680 cm^{-1}), but the correlation is less obvious than the 18:3*c*Δ9,12,15, which is hardly surprising given the low abundance in the sample and the corresponding high prediction error. The weighting plot for 18:1*c*Δ9 is complicated by the occurrence of strong negative and positive components, which, although they presumably arise from changes in saturation from the mean values, are so close to those values (18:1*c* is the predominant FA in adipose samples) that the model can only find a very complex relationship between the abundance of 18:1*c* and the spectra.

Surprisingly good predictions were obtained for a number of the less abundant FA, with 15:0 and 17:0 giving R^2 = 0.82 and RMSEP = 10.5% of the range, despite being present in relative abundances of 0.5% of the total FA content. It seems highly unlikely that these low-abundance compounds give distinct characteristic signals that are detectable under our experimental conditions, since the intensity of even the strongest bands in a FA present at <1% would be similar to the noise in the data, and the differences that would allow the particular FA to be distinguished from similar compounds in the tissue would be expected to be much smaller again. A more convincing explanation is that this good modeling ability arises from an underlying correlation between the low-abundance FA and much more abundant ones whose signals would be expected to be detectable. Since the adipose tissue is a product of biosynthetic pathways, such cross-correlation might be expected. In this study the samples were dissected from four animal species (two ruminant and two nonruminant) with a selection of breeds from within each species to minimize cross-correlation. Moreover, a range of experimental programs and commercial suppliers was used to reduce the influence of feeding regimes. The consequence is that the cross-correlation is significantly less than that in the butterfat samples previously studied (18), so the correlation determined within this sample set is more widely applicable.

One way of explicitly including the cross-correlation in the analysis and simplifying the data is to carry out a principal components analysis (PCA) and divide all the FA into groups according to which others their abundance correlates with. Figure 4 shows such a plot for the FA in this study. The FA abundances for each of the five groups found in the PCA analysis of the data were then summed, and the Raman spectra were used to model the variation between the FA groups. The results of these regressions of the FA groups are summarized in Table 4, with details of contributing FA given in the footnote. The one obvious group is the FA set comprising 18:2*t*Δ9,12; 18:1*c*Δ9; 18:3Δ6,9,12; 12:0; and 16:1*c*Δ9 while another large group contains highly *cis* unsaturated compounds 18:2*c*Δ9,12, 18:3*c*Δ9,12,15, and 20xa (which is one of the unassigned 20-carbon unsaturated FA). The Raman spectra were able to predict the total abundance of all of these groups with some success. In fact, the least well-modeled group is the one constituting the largest fraction of the sample, although this may be attributed to the lower range of values relative to the mean abundance (range < 0.66 σ) that this group shows (in the remaining groups the range was >1.5 σ).

A further useful group that can be defined, though not cross-correlated by relative abundance, is the combined proportion of PUFA. This group of FA, as detailed above, is of extreme interest because of their relevance to health issues. Raman spectroscopy was able to model this group well (R^2 = 0.97, RMSEP = 4.0% of 4 σ). One individual FA that is of particular interest is the EFA 18:3*c*Δ9,12,15, which was well modeled (R^2 = 0.932) with good prediction accuracy (7.6% of 4 σ). Using a PLS1 regression allows models to be optimized for any given FA. In this case, using PLS1 regression to predict 18:3*c*Δ9,12,15 gave a slightly better result than PLS2 (R^2 = 0.946, RMSEP = 5.8% of 4 σ). As already alluded to, Raman spectroscopy is able to predict the relative abundances of several FA that influence the level of cholesterol in the blood including 14:0 and 16:0, which increase cholesterol, and the unsaturated FA, which are important in reducing cholesterol. Unfortunately the limitations of the GC method used did not allow calculation of the cholesterolemic index, but the results suggest that Raman could be used to predict this important parameter. One FA of interest, CLA, was not detected in large quantities in concentrate-fed ruminants, most probably because it was not sufficiently resolved from the more abundant 18:3Δ9,12,15

on the GC column used in this study. However, it has been previously demonstrated that Raman spectroscopy can be used to predict the relative abundance of CLA in butterfats from grass-fed cows, where higher concentrations are found (18).

Overall, the prediction ability for the FA in this study on adipose tissue (average R^2 = 0.74 and average RMSEP = 12.0% of 4 σ for the 18 most abundant FA) was significantly better than was found in experiments carried out on clarified butter samples analyzed at 55°C [average R^2 = 0.68, and average RMSEP = 18.5% of 4 σ for the 18 most abundant FA (18)]. This improvement is not due to higher signal-to-noise ratios in the adipose spectra but seems to stem from the fact that the spectra of the adipose tissue were recorded at temperatures within the melting range whereas those of the butterfat were recorded on fully melted samples (although the slightly larger range of abundances for the FA in the adipose samples may also have contributed). Since the Raman spectrum of each FA changes with physical state, recording spectra in a temperature range that allows the adoption of different physical states, i.e., within the melting range, gives information that is simply lost at temperatures where all the components have melted. In this case the adipose tissue was run at 21 ± 2°C (ambient temperature), which allowed the higher m.p. TG to solidify and give rise to characteristic sharp bands that can easily be distinguished from the broader bands of the liquid constituents (shorter-chain or unsaturated components).

The results shown in Table 4 compare favorably with other published investigations that used spectroscopic techniques to predict FA composition. A number of papers investigating the use of NIR spectroscopy to predict FA composition of foodstuffs (21–24) found that it is possible to predict the proportion of the major unsaturated FA well (R^2 typically ≥0.95 for the most abundant unsaturated FA) but that the prediction ability is reduced as the proportion of the FA decreases and the saturation increases. Velasco *et al.* (23) found the NIR regression correlation coefficients for saturated FA such as palmitic and stearic acids in rapeseed were lower (<0.8) that those for unsaturated FA, which were between 0.84 and 0.98 (25). Kohler and Kallweit (21) found that the NIR regression correlation coefficients for the 15 major FA in sheep intramuscular fat ranged from r = 0.57 to 0.90 (R^2: 0.32–0.81). When FTIR was used to predict the FA composition of dissected but unextracted adipose tissue (26) it gave poor correlation coefficients for the main FA (R^2 = 0.69–0.79) although much better correlations (R^2 = 0.91–0.98) were found if the tissue was extracted before analysis. Similarly, NIR analysis had poorer prediction ability for the less significant FA compared with Raman analysis (21).

It is clear that Raman has the advantage of giving correlation coefficients as high as the best of the other spectroscopic methods, and it can do this without the need for prior solvent extraction steps in the analysis. The most common method of determining the FA profile of adipose tissue and similar TG systems is to use GC; typically, 100-m capillary columns and temperature ramps are required to obtain effective separation and identification of isomers. Since this GC method requires time-consuming, destructive sample extraction and transmethylation, the ability to use Raman spectroscopy, with a simple calibration, on unextracted, dissected tissue is a significant advantage.

Thus, Raman spectroscopy can accurately predict the bulk properties of adipose tissue and a detailed FA profile of the 18 most abundant FA found in neat adipose tissue with an accuracy at least as good as that of other spectroscopic methods but with extremely straightforward sampling. The bulk unsaturation parameters could be predicted successfully (*cis*: RMSEP = 4.7% of 4 σ; total PUFA RMSEP = 4.0% of 4 σ) but *trans* unsaturation was not so well modeled (RMSEP = 18% of 4 σ). For the individual FA, the average RMSEP of the 18 most abundant FA was 11.9% of 4 σ while the prediction errors for the five most abundant FA were all better than the average value (in some cases as low as RMSEP = 4.7% of 4 σ). Of particular note was the ability of Raman spectroscopy to predict quantities important in human health, such as the proportion of 18:3*c*Δ9,12,15 present, or the total proportion of PUFA. The accuracy of the prediction, although as good as other spectroscopic methods, does not approach that of conventional GC methods: This method is not intended as an alternative to established chromatographic methods for high-accuracy profiling. The approach is predominantly aimed at on-line applications, in which the lower accuracy is compensated by the ability to make rapid, noncontact measurements with no additional sample preparation.

ACKNOWLEDGMENTS

J.R.B. wishes to thank the Department of Agriculture and Rural Development for Northern Ireland for the provision of a post-graduate studentship to undertake this work and for the facilities provided at the Agriculture and Food Science Centre, Belfast.

REFERENCES

1. Anon. (1994) Nutritional Aspects of Cardiovascular Disease, Report on Health and Social Subjects No. 46, Her Majesty's Stationery Office (HMSO), London.
2. Keys, A., Anderson, J.T., and Grande, F. (1965) Serum Cholesterol Response to Changes in the Diet IV. Particular Saturated Fatty Acids in the Diet, *Metabolism 14*, 776–787.
3. Mattson, F.H., and Grundy, S.M. (1985) Comparison of the Effects of Dietary Saturated, Monounsaturated and Polyunsaturated Fatty Acids on Plasma Lipids and Lipoproteins in Man, *J. Lipid Res. 26*, 192–204.
4. Mensink, R.P., and Katan, M.B. (1992) Effect of Dietary Fat on Lipids and Lipoproteins: A Meta-analysis of 27 Trials, *Arterioscler. Thromb. 12*, 911–919.
5. Kris-Etherton, P.M., and Yu, S. (1997) Individual Fatty Acid Effects on Plasma Lipids and Lipoproteins: Human Studies, *Am. J. Clin. Nutr. 65*, 1628S–1644S.
6. Vanschoonbeek, K., de Maat, M.P.M., and Heemskerk, J.W.M. (2003) Fish Oil Consumption and Reduction of Arterial Disease, *J. Nutr. 133*, 657–660.
7. Pariza, M.W., and Hargreaves, W.A. (1985) A Beef-Derived Mutagenesis Modulator Inhibits Initiation of Mouse Epidermal Tumours by 7,12-Dimethylbenz[a]anthracene, *Carcinogenseis 6*, 591–593.
8. Belury, M.A., and Vanden Heuvel, J.P. (1997) Protection Against Cancer and Heart Disease by the Dietary Fat, Conju-

gated Linoleic Acid: Potential Mechanisms of Action, *Nutr. Dissert. Update J. 1*, 59–63.
9. Ip, C. (1997) Review of the Effects of *trans* Fatty Acids, Oleic Acid, n-3 Polyunsaturated Fatty Acids and Conjugated Linoleic Acid on Mammary Carcinogenesis in Animals, *Am. J. Clin. Nutr. 66*, 1523S–1529S.
10. Kritchevsky, D. (1997) Conjugated Linoleic Acid and Experimental Atherosclerosis in Rabbits, in *Advances in Conjugated Linoleic Acid Research Vol. 1* (Yurawecz, M.P., Mossoba, M.M., Kramer, J.K.G., Pariza, M.W., and Nelson, G.J., eds.), pp. 397–403, AOCS Press, Champaign.
11. Demeyer, D., and Doreau, M. (1999) Targets and Procedures for Altering Ruminant Meat and Milk Lipids, *Proc. Nutr. Soc. 58*, 593–607.
12. Jimenez-Colmenero, F., Carballo, J., and Cofrades, S. (2001) Healthier Meat and Meat Products: Their Role as Functional Foods, *Meat Sci. 59*, 5–13.
13. Gulati, S.K., May, C., Wynn, P.C., and Scott, T.W. (2002) Milk Fat Enriched in n-3 Fatty Acids, *Anim. Feed Sci. Technol. 98*, 143–152.
14. Fearon, A.M., Mayne, C.S., Beattie, J.A.M., and Bruce, D.W. (2004) Effect of Level of Oil Inclusion in the Diet of Dairy Cows at Pasture on Animal Performance and Milk Composition and Properties, *J. Sci. Food Agric. 84*, 497–504.
15. Beattie, J.R., Bell, S.J., and Moss, B.W. (2004) A Critical Evaluation of Raman Spectroscopy for the Analysis of Lipids: Fatty Acid Methyl Esters, *Lipids 39*, 407–419.
16. Oakes, R.E., Beattie, J.R., Moss, B., and Bell, S.E.J. (2002) Conformations, Vibrational Frequencies and Raman Intensities of Short Chain Fatty Acid Methyl Esters Using DFT with 6-31 G(d) and Sadlej pVTZ Basis Sets, *J. Mol. Struct. THEOCHEM 586*, 91–110.
17. Oakes, R.E., Beattie, J.R., Moss, B.W., and Bell, S.E.J. (2003) DFT Studies of Long-Chain FAMEs: Theoretical Justification for Determining Chain Length and Unsaturation from Experimental Raman Spectra, *J. Mol. Struct. THEOCHEM 626*, 27–45.
18. Beattie, J.R., Bell, S.E.J., Borgaard, C., Fearon, A.M., and Moss, B.W. (2004) Multivariate Prediction of Clarified Butter Composition Using Raman Spectroscopy, *Lipids 39*, 897–906.
19. Beattie, R.J., Bell, S.J., Farmer, L.J., Moss, B.W., and Desmond, P.D. (2004) Preliminary Investigation of the Application of Raman Spectroscopy to the Prediction of the Sensory Quality of Beef Silverside, *Meat Sci. 66*, 903–913.
20. Bailey, G.F., and Horvat, R.J. (1972) Raman Spectroscopy Analysis of the *cis/trans* Isomer Composition of Edible Vegetable Oils, *J. Am. Oil Chem. Soc. 49*, 494–498.
21. Kohler, P., and Kallweit, E. (1999) Determination of Fatty Acid Composition of Intramuscular Fat in Sheep by Near-Infrared Transmission Spectroscopy (NIT) and Their Importance for the Meat Production, *Agribiol. Res.–Z. Agrarbiol. Agrikulturchem. Okol. 52*, 145–154.
22. Sato, T., Takahashi, M., and Matsunaga, R. (2002) Use of NIR Spectroscopy for Estimation of FA Composition of Soy Flour, *J. Am. Oil Chem. Soc. 79*, 535–537.
23. Velasco, L., Mollers, C., and Becker, H.C. (1999) Estimation of Seed Weight, Oil Content and Fatty Acid Composition in Intact Single Seeds of Rapeseed (*Brassica napus* L.) by Near-Infrared Reflectance Spectroscopy, *Euphytica 106*, 79–85.
24. Molette, C., Berzaghi, P., Zotte, A.D., Remignon, H., and Babile, R. (2001) The Use of Near-Infrared Reflectance Spectroscopy in the Prediction of the Chemical Composition of Goose Fatty Liver, *Poult. Sci. 80*, 1625–1629.
25. Velasco, L., and Becker, H.C. (1998) Estimating the Fatty Acid Composition of the Oil in Intact-Seed Rapeseed (*Brassica napus* L.) by Near-Infrared Reflectance Spectroscopy, *Euphytica 101*, 221–230.
26. Ripoche, A., and Guillard, A.S. (2001) Determination of Fatty Acid Composition of Pork Fat by Fourier Transform Infrared Spectroscopy, *Meat Sci. 58*, 299–304.
27. Sadeghi-Jorabchi, H., Hendra, P.J., Wilson, R.H., and Belton, P.S. (1990) Determination of the Total Unsaturation in Oils and Fats by Fourier Transform Raman Spectroscopy, *J. Am. Oil Chem. Soc. 67*, 483–486.
28. Chmielarz, B., Bajdor, K., Labudzinska, A., and Klukowskamajewska, Z. (1995) Studies on the Double-Bond Positional Isomerization Process in Linseed Oil by UV, IR and Raman-Spectroscopy, *J. Mol. Struct. 348*, 313–316.
29. Butler, M., Salem, N., Hoss, W., and Spoonhower, J. (1979) Raman Spectral Analysis of the 1300 cm^{-1} Region for Lipid and Membrane Studies, *Chem. Phys. Lipids 29*, 99–102.
30. Snyder, R.G., Cameron, D.G., Casal, H.L., Compton, D.A.C., and Mantsch, H.H. (1982) Studies on Determining Conformational Order in *n*-Alkanes and Phospholipids from the 1130 cm^{-1} Raman Band, *Biochim. Biophys. Acta 684*, 111–116.
31. Lawson, E.E., Anigbogu, A.N.C., Williams, A.C., Barry, B.W., and Edwards, H.G.M. (1998) Thermally Induced Molecular Disorder in Human Stratum Corneum Lipids Compared with a Model Phospholipid System; FT-Raman Spectroscopy, *Spectrochim. Acta A:Mol. Biomol. Spectros. 54*, 543–558.
32. Susi, H., Sampugna, J., Hampson, J.W., and Ard, J.S. (1979) Laser-Raman Investigation of Phospholipid-Polypeptide Interactions in Model Membranes, *Biochemistry 18*, 297–301.
33. Kint, S., Wermer, P.H., and Scherer, J.R. (1992) Raman-Spectra of Hydrated Phospholipid-Bilayers. 2. Water and Headgroup Interactions, *J. Phys. Chem. 96*, 446–452.

[Received July 8, 2005; accepted February 16, 2006]